Schizosaccharomyces pombe Rtf2 mediates site-specific replication termination by inhibiting replication restart

Takabumi Inagawa[a,1], Tomoko Yamada-Inagawa[a,1], Trevor Eydmann[a], I. Saira Mian[b], Teresa S. Wang[c], and Jacob Z. Dalgaard[a,2]

[a]Marie Curie Research Institute, The Chart, Oxted, Surrey RH8 0TL, United Kingdom; [b]Life Sciences Division, Mail Stop 74-197, Lawrence Berkeley National Laboratory, 1 Cyclotron Road, Berkeley, CA 94720-8265; and [c]Department of Pathology, Stanford University School of Medicine, Stanford, CA 94305-5324

Edited by Marlene Belfort, New York State Department of Health, Albany, NY, and approved March 16, 2009 (received for review December 7, 2008)

Here, we identify a phylogenetically conserved *Schizosaccharomyces pombe* factor, named Rtf2, as a key requirement for efficient replication termination at the site-specific replication barrier *RTS1*. We show that Rtf2, a proliferating cell nuclear antigen-interacting protein, promotes termination at *RTS1* by preventing replication restart; in the absence of Rtf2, we observe the establishment of "slow-moving" Srs2-dependent replication forks. Analysis of the *pmt3* (SUMO) and *rtf2* mutants establishes that *pmt3* causes a reduction in *RTS1* barrier activity, that *rtf2* and *pmt3* are nonadditive, and that *pmt3* (SUMO) partly suppresses the *rtf2*-dependent replication restart. Our results are consistent with a model in which Rtf2 stabilizes the replication fork stalled at *RTS1* until completion of DNA synthesis by a converging replication fork initiated at a flanking origin.

proliferating cell nuclear antigen | *RTS1* | SUMO | Srs2 | Rtf1

Stalling of replication forks at damaged bases, at bound factors, caused by dysfunctional replication enzymes or low levels of deoxyribonucleotides, can result in genome instability and, in higher organisms, can lead to the development of cancer or premature aging. However, several cellular processes ensure the completion of S phase when replication barriers are encountered. First, the intra-S phase checkpoint has been shown to play a central role in preventing the collapse of stalled replication forks (1–3). Second, several cellular processes allow restart of DNA synthesis when forks are stalled at barriers. These processes include (*i*) the "error-free bypass," involving regression of the collapsed replication fork and the formation of a Holliday junction, which allows the newly synthesized lagging strand to act as template for bypassing a lesion in the leading-strand template (4, 5); (*ii*) "translesion DNA synthesis," involving the recruitment of error-prone polymerases, which can synthesize past lesions, to the stalled replication fork (6, 7); (*iii*) "direct nascent leading-strand restart" recently described in bacteria, where de novo priming of leading-strand synthesis occurs (8); (*iv*) "break-induced replication," a process mediated by nucleases that recognize and cleave collapsed and/or regressed forks (9). The cleavage reaction leads to the formation of a new 3′-end that after strand invasion, mediated by recombinases, is used to establish a novel replication fork.

Several site-specific replication barriers are described where replication forks are purposefully stalled and replication is terminated. Such barriers are described at telomeres, centromeres, tRNA genes, in rDNA arrays and at the *Schizosaccharomyces pombe* mating-type locus (10). An interesting question that remains to be answered is what mechanisms and processes act to prevent the replication restart pathways described above from acting when replication forks are stalled at site-specific barriers.

The *RTS1* element is such a site-specific replication barrier. This genetic element is located in the mating-type region at the *cen2*-proximal side of *mat1*. *RTS1* acts to ensure efficient mating-type switching by regulating the direction of replication (11, 12); *S. pombe* switches mating type through a replication-coupled recombination event that depends on *mat1* being replicated in a specific direction [supporting information (SI) Fig. S1]. *RTS1* is a polar barrier, terminating replication forks moving in the *cen2*-distal direction. *RTS1* is related to the class of site-specific replication barriers also found in the eukaryotic rDNA gene arrays (13). The *cis*-acting sequences of the element consist of (*i*) a ≈450-bp long region B that contains four repeated ≈60-bp conserved motifs, each of which possesses replication barrier activity, and (*ii*) region A that acts to enhance the activity of region *B*, mediating an ≈4-fold increase in barrier activity. We have shown that there are four *trans*-acting replication factors, Swi1, Swi3, Rtf1, and Rtf2, involved in the termination process at *RTS1* (13). Swi1 and Swi3 travel with the replication fork, whereas Rtf1 in vitro has been shown to interact directly with both *RTS1* regions A and B (10). Rtf1 is homologous to the *S. pombe* Reb1 and to mouse and human TTF1 proteins required for barrier function at the corresponding rDNA barriers. Furthermore, an epistasis analysis has established that Rtf2 acts downstream from Rtf1 and is required for region A enhancer activity (13). Here, we identify Rtf2 as the defining member of a new family of factors that is conserved from yeast to humans, and we show that Rtf2 acts to prevent replication restart.

Results

Identification of Rtf2. Rtf2 complementation group was identified in a genetic screen that took advantage of the dependence of *S. pombe* mating-type switching mechanism on a specific direction of replication at the *mat1* locus (11, 14). Of the four genetic complementation groups identified, *swi1*, *swi3*, *rtf1*, and *rtf2*, the *rtf2* group contained only one allele named *rtf2-1* (*SI Materials and Methods*). The *rtf2* gene was isolated by complementation of the *rtf2-1* sporulation phenotype using a plasmid library and was subsequently identified as the ORF SPAC1D4.09C by sequencing. The identity was verified by plasmid integration followed by a genetic linkage analysis and by the construction of a Δ*rtf2* mutation (Fig. 1 *A* and *B* and *SI Materials and Methods*). Furthermore, an *rtf2* cDNA clone was isolated and sequenced, establishing the presences of three introns (Fig. S2). Also, the

Author contributions: T.I., T.Y.-I., I.S.M., T.S.W., and J.Z.D. designed research; T.I., T.Y.-I., T.E., I.S.M., and J.Z.D. performed research; T.I., T.Y.-I., I.S.M., and J.Z.D. analyzed data; and T.I., T.Y.-I., and J.Z.D. wrote the paper.

The authors declare no conflict of interest.

This article is a PNAS Direct Submission.

Data deposition: The sequence reported in this paper has been deposited in the GenBank database (accession no. FN376423).

[1]T.Y. and T.Y.-I. contributed equally to this work.

[2]To whom correspondence should be addressed. E-mail: j.dalgaard@mcri.ac.uk.

This article contains supporting information online at www.pnas.org/cgi/content/full/0812323106/DCSupplemental.

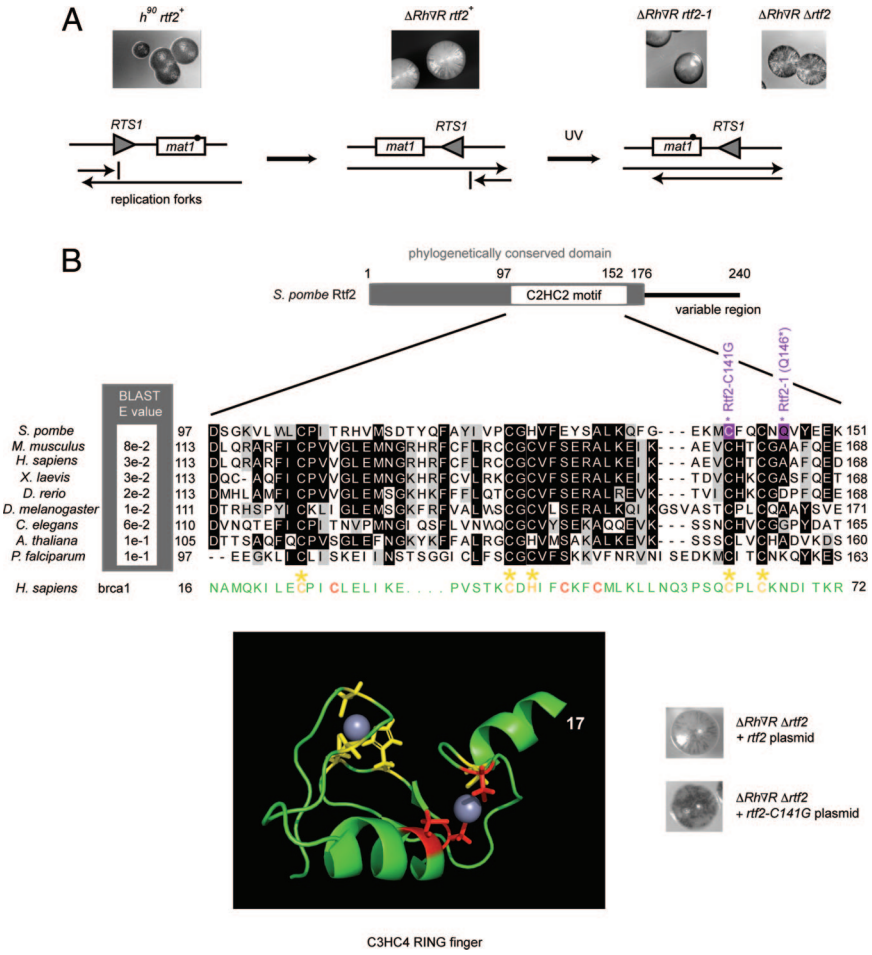

Fig. 1. *Rtf2* is the defining member of a new protein family. (*A*) Schematic drawing of the genetic screen used for identification of the *rtf2* gene. (*Left*) Wild-type cells. The *RTS1* element terminates replication forks that are moving in the *cen2*-distal direction while allowing forks moving in the *cen2*-proximal direction to pass through the region. A pictograph inserted above displays wild-type (h^{90} $rtf2^{+}$) sporulating colonies staining dark after treatment with iodine vapors. Iodine vapors stain starch present in the *S. pombe* spores. (*Middle*) Transposing (horizontal arrow) the *RTS1* element, while inverting it in the process, from the *cen2*-proximal side of *mat1* to the *cen2*-distal side changes the direction the *mat1* locus is replicated and leads to the abolishment of *mat1* imprinting and, as a consequence, mating-type switching, mating, meiosis, and sporulation. Pictograph above displays the yellow iodine staining phenotype characteristic of colonies formed by this nonsporulating strain (JZ183; Δ*RTS1-mat1-SspI*::*inv-RTS1*). (*Right*) UV mutagenesis (second horizontal arrow) of genes encoding factors required for *RTS1* function leads to loss of *RTS1* barrier function and therefore to a partial restoration of the wild-type direction of replication at *mat1*. As a consequence, *mat1* imprinting, switching, mating, meiosis, and sporulation are also partly restored. Thus, in Δ*RTS1-mat1-SspI*::*inv-RTS1* genetic background *RTS1* replication–barrier activity can be measured by quantification of sporulation. Sporulating colonies of the isolated *rtf2-1* strain (JZ230) and the constructed Δ*rtf2* strain (SC10) display an intermediate staining phenotype (*Inset pictures*). Genotypes of strains are displayed above the *Inset pictures*. (*B*) Graphic outline of the conserved domains of Rtf2. The Rtf2 contains the C2HC2 motif related to the C3HC4 RING-finger motif. (*Top*) Graphic outline of the Rtf2 sequence displaying the positions of the phylogenetically conserved segment defined by Pfam DUF602 (gray box; Fig. S3) and the C2HC2 motif. (*Middle*) Sequence alignment of the C2HC2 motif from Pfam DUF602 sequence members. The GenBank accession numbers are: *Mus musculus*, NP_079818; *Homo sapiens*, CA_C03740; *Danio rerio*, NP_956036; *Xenopus laevis*, AAH54212; *Caenorhabditis elegans*, NP_609443; *Arabidopsis thaliana*, NP_200610; *Plasmodium falciparum*, NP_704807. The *H. sapiens* BRCA1 sequence shown in green below the alignment contains the related C3HC4 RING-finger motif (accession number AAH85615). The C3HC4 residues of this motif that in the solution structure act to chelate the two Zn^{2+} ions are highlighted in red and yellow (31); the yellow residues are shared with the C2HC2 motif. Inserted tertiary fold displays the peptide backbone and chelating side chains of the BRCA1 segment given in the alignment. (*Inset pictures*) *rtf2-C141G* point mutation abolishes the ability of an Rtf2-expressing plasmid (pTE201) to complement the *rtf2-1* phenotype (strain JZ230) observed in the genetic assay described in *A*.

rtf2-1 allele was identified as a nonsense mutation at amino acid position Q146* (Fig. 1*B* and Fig. S2). A computational analysis of the Rtf2 amino acid sequence established that Rtf2 is the founding member of a protein family that is conserved from fission yeast to humans (Fig. 1*B* and Fig. S3). Interestingly, this protein family is characterized by a C2HC2 motif similar to C3HC4 RING-finger motif known to bind Zn^{2+} ions and mediate protein–protein interactions (15). Importantly, the C2HC2 motif lacks three of the seven conserved cysteines of the C3HC4 motif. The C3HC4 RING-finger motif can bind two Zn^{2+} ions, as shown for the human BRCA1 protein (Fig. 1*B*). The two Zn^{2+} ions are chelated at two binding sites each constituted by four of the eight conserved C3HC4 residues. An alignment of the Rtf2 protein sequence with known C3HC4 motifs suggests that the Rtf2 sequence folds up, creating a RING finger-like structure while forming only one functional Zn^{2+} ion-binding site.

***rtf2* Mutation Causes an Increase in Large-Y Intermediates.** When comparing the 2D gel signals of the *RTS1* element observed in the *rtf2-1* and Δ*rtf2* genetic backgrounds with those observed in the wild-type background, we noticed an increase in the intensity of the descending part of the Y-arc (Fig. 2). The descending arc consists of the large-Y DNA structures formed after the replication fork has passed the *RTS1* element. One possibility is that the increase of this signal is caused by the appearance of slow-moving replication forks established by nonprocessive repair polymerase through replication restart pathways; or, alternatively, the processivity of the restarted replication forks are changed. In either case, Rtf2 acts to prevent such restart of the replication forks that have undergone an Rtf1-dependent stalling at *RTS1*. To test this model more carefully, we analyzed known *S. pombe* mutations that affect restart pathways at stalled and collapsed replication forks.

***srs2*, but Not *rqh1*, Is Required for Restart of Replication at *RTS1*.** As outlined in the Introduction, two helicases play a key role at stalled replication forks; Rqh1 is the *S. pombe* RecQ homolog, which acts by reversing regressed replication forks as part of the error-free bypass pathway (5), whereas Srs2 is a key regulatory factor, implicated in replication fork stability (9, 16). Srs2 is a 3′ to 5′ helicase structurally related to bacterial UvrD and Rep DNA helicases that act by removing the ssDNA-binding protein Rhp51 from nucleofilaments (17, 18). To analyze the involvement of these two helicases in replication events at *RTS1*, we first compared the *RTS1* barrier activity in wild-type, Δ*rtf2*, Δ*srs2*, and Δ*rtf2* Δ*srs2*. The Δ*srs2* mutation did not affect the *RTS1* barrier activity in the $rtf2^{+}$ background, although a minor increase in the intensity of the part of the Y-arc that is constituted by large-Y intermediates is observed. However, analysis of the double

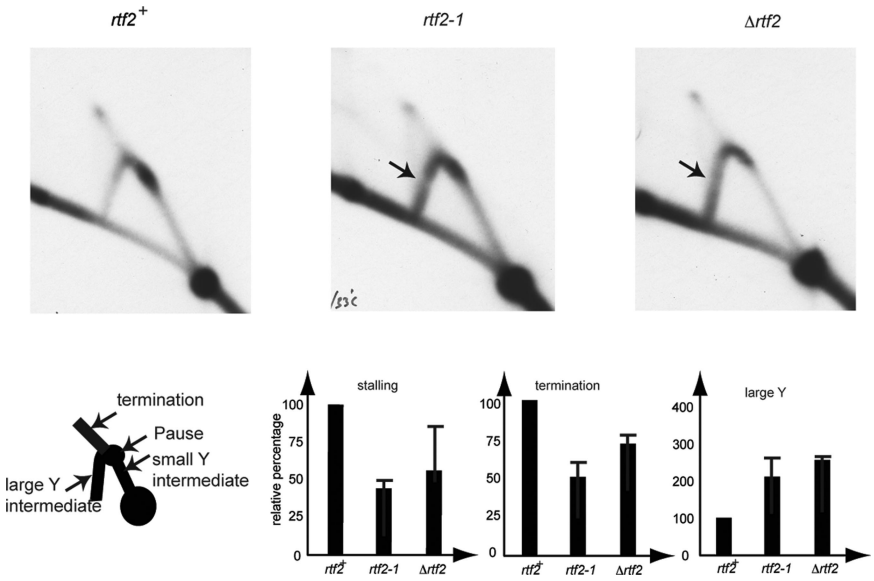

Fig. 2. Rtf2 is required for efficient replication termination at *RTS1*. Quantification of the effect of the *rtf2-1* and Δ*rtf2* alleles on *RTS1* barrier activity (plasmid pBZ142) using 2D gel analysis of replication intermediates is shown. Strains JZ183, JZ230, and SC10 were grown at 33 °C. Replication intermediates were purified, digested with SacI and PstI restriction enzymes, separated on 2D gels, and analyzed by Southern blotting using a probe specific to the *RTS1* element. Pausing (the signal is defined in the inserted drawing at *Lower Left*), termination, and the large-Y signals were quantified by using a Bio-Rad PhosphorImager. A comparison of the intensities of the observed termination, pause, and large-Y signals is given below in the inserted graphs. The values were standardized by using the intensity of the ascending Y-arc and are displayed as the relative percentage of the wild-type signals. Mean and largest measurement from two experiments are shown.

mutant showed that Δ*srs2* almost completely suppressed the Δ*rtf2* mutation with regard to pausing and termination at *RTS1* and restored the level of large-Y intermediates to wild-type levels (Fig. 3*B*). These data suggested that in the Δ*rtf2* genetic background Srs2 is required for restart of replication involving the formation of slow-moving replication forks at *RTS1*. In contrast to this finding, neither the *rqh1* single mutant nor the *rqh1 rtf2-1* double mutant affected *RTS1* replication barrier activity as measured by pause site intensity and by termination intermediate intensity on 2D gels (Fig. S4). However, we did observe an increased slow growth and elongated-cell phenotype in the Δ*rtf2* Δ*rqh1* strain compared with the Δ*rqh1* single mutant, suggesting that these two gene products have overlapping roles for maintaining genome stability.

Polκ, Polη, and Polζ Are Not Required for the Establishment of Slow-Moving Replication Forks. *Saccharomyces cerevisiae* Srs2 acts with mutagenic repair polymerases as part of the translesion synthesis pathway acting at collapsed replication forks (19, 20). Three of the repair polymerases known to act in this pathway are Polη, Polκ, and Polζ (6). We therefore constructed the double-mutant strains Δ*rtf2*Δ *polη*, Δ*rtf2* Δ*polκ*, and Δ*rtf2* Δ*polζ* and the quadruple mutant strain Δ*rtf2*Δ*polζ* Δ*polκ* Δ*polη*. When the replication barrier activity was analyzed, there were no significant decreases in the intensity of the descending part of the arc constituted by large-Y structures (Fig. 3*B*). Thus, the error-prone polymerases Polη, Polκ, and Polζ in the Δ*rtf2* mutant background do not act at *RTS1* to restart replication.

Rtf2 Interacts with Proliferating Cell Nuclear Antigen (PCNA). To start addressing the molecular mechanism by which Rtf2 mediates replication termination, we first analyzed the subcellular localization of Rtf2 in both living and fixed cells. For this purpose we used GFP- or 13Myc-tagged Rtf2 strains, respectively. Neither of these tags affects the Rtf2 function in our genetic assay. The analysis revealed that both GFP-tagged Rtf2 and 13Myc-tagged Rtf2 display a predominantly nuclear localization (Fig. 4*A*). Because of the central role of PCNA in regulating molecular events at stalled replication forks, the nuclear localization of Rtf2, and the role of this protein at *RTS1*, we proceeded to investigate whether Rtf2 and PCNA interact directly. Using *S. cerevisiae* two-hybrid analysis, we detected a weak interaction between Rtf2 and PCNA (Fig. 4*B Upper*). To verify that this interaction occurred in vivo, we performed pull-down assays of PCNA by using extracts from strains carrying either His_6-tagged PCNA and 13Myc-tagged Rtf2 or His_6-tagged PCNA and GST-tagged Rtf2. In both cases, Rtf2 was pulled down with PCNA. Control experiments excluded independent Rtf2-13Myc binding to the nickel resin used (Fig. 4*C Lower*). Similarly, DNase digestion using MNase excluded that the copurification was caused by both PCNA and Rtf2 interacting with DNA (Fig. 4*C Lower*). However, although the Rtf2 protein is abundant in the crude extracts, we only detected a weak Rtf2 signal in our pull-down assays compared with the intense PCNA signal. Thus, the data suggest that although Rtf2 and PCNA interact, the interaction is weak or transient, or only occurs at a subset of replication forks.

To establish whether the detected Rtf2–PCNA interaction is of functional importance for Rtf2 activity at *RTS1*, we took a genetic approach. Zn^{2+} finger motifs have been proposed to have a general role in mediating protein–protein interactions (21). We therefore introduced a substitution of one of the putative "Zn^{2+}"-chelating residues in Rtf2 by using site-directed mutagenesis (Rtf2-C141G, Fig. 1*B*). Using our genetic assay, we found that the obtained C141G mutation reduced the ability of the protein to complement the *rtf2-1* mutation, suggesting that the C2HC2 motif is at least partly required for Rtf2 function (Fig. 1*B Lower Right*). Furthermore, using both the two-hybrid assay and the coimmunoprecipitation assay we established that the Rtf2-C141G mutation also abolished the ability of the protein to interact with PCNA (Fig. 4*C Lower*). However, it should be noted that although Rtf2-C141G did not affect the protein levels in our two-hybrid assay, a reduction in protein levels was observed when the mutation was introduced into the *S. pombe* genome. In summary, Rtf2 is a PCNA-interacting factor, and the interaction requires the Rtf2-C141G residue present in the putative Zn^{2+}-binding motif.

Sumo (Pmt3) Is Required for Replication Termination at the *RTS1* Element. Sumoylation of *S. cerevisiae* PCNA at residue K164 acts to stabilize replication forks stalled at sites of DNA damage, as well as to mediate the recruitment of Srs2 and translesion polymerases (19, 20, 22). Also, *S. pombe* PCNA is sumoylated in an S phase that is perturbed by DNA damage (23). We speculated that Rtf2 might affect the sumoylation of PCNA at stalled replication forks. An analysis of the *rtf2-1* and Δ*rtf2* strains detected a slight sensitivity to alkylation damage, but not hydroxyurea, UV light, or camptothecin, suggesting that Rtf2 plays only a minor role at stalled replication forks at damaged bases,

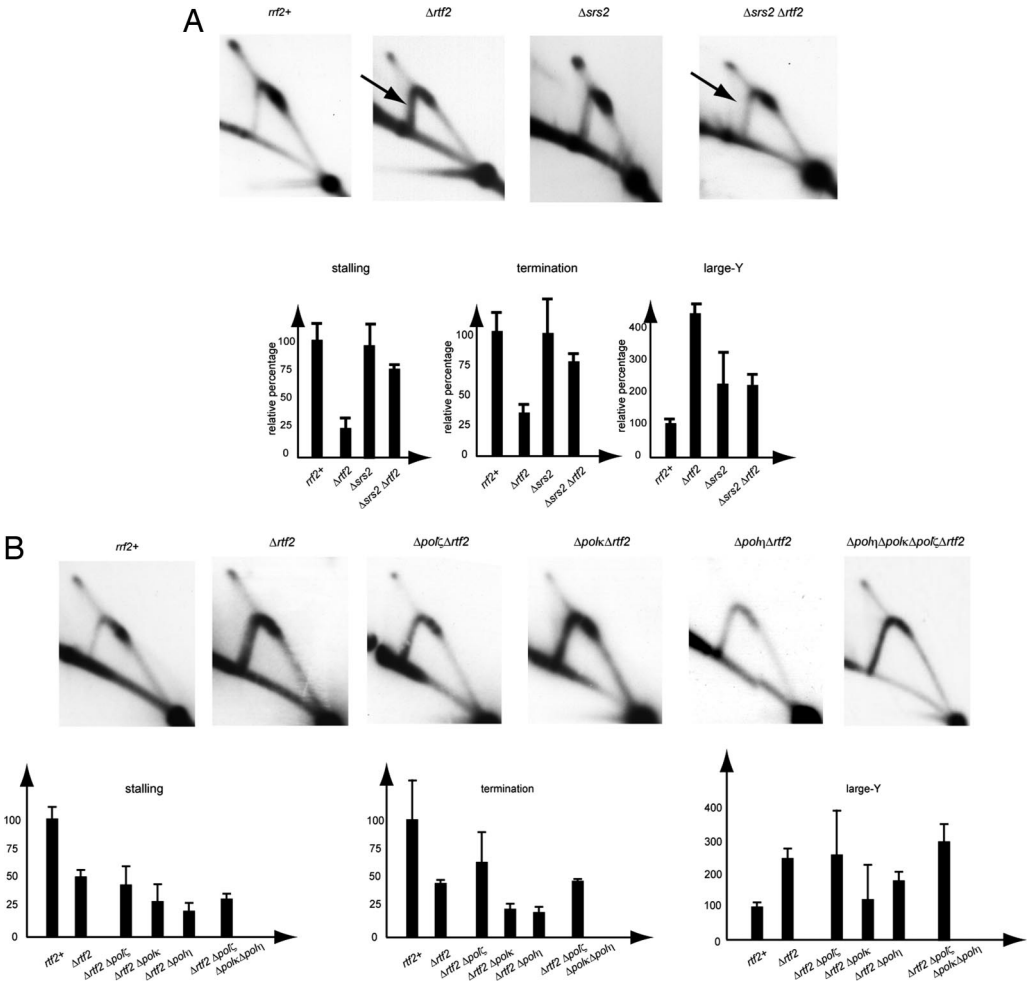

Fig. 3. Analysis of replication restart in the *rtf2* genetic background. (*A*) The Δ*srs2* mutation partly restores *RTS1* barrier activity in the Δ*rtf2* genetic background. Two-dimensional gel analysis of *RTS1* replication intermediates (plasmid JZ142) from Δ*srs2* (FO1117) single-mutant strain and Δ*rtf2* Δ*srs2* (TISP249) double-mutant strain is shown. Inserted graphs display the relative intensity of the observed pause, termination, and large-Y signals, quantified as described in Fig. 2 legend. Two independent experiments were conducted, thus, mean and largest value are displayed for each measurement. (*B*) The Δ*polη*, Δ*polκ*, and Δ*polζ* mutations do not complement the observed decrease in the *RTS1* barrier activity observed in the Δ*rtf2* mutant background. Two-dimensional gel analysis of *RTS1* region B (pSC11) replication intermediates in wild-type (JZ472), and Δ*rtf2* Δ*polη* (TY241), Δ*rtf2* Δ*polζ* (TY234), Δ*rtf2* Δ*polκ* (TY235) double-mutant and Δ*rtf2* Δ*polη* Δ*polζ* Δ*polκ* (TY285) quadruple mutant strains are shown. Inserted graphs display the relative intensity of the observed pause, termination and large-Y signals to those of the wild-type signals (displayed to the *Left* in *A*). Signals were quantified as described for *B* and Fig. 2.

in the DNA damage response, or in repair generally (Fig. S5). We therefore investigated whether Pmt3 (the *S. pombe* SUMO homolog) is directly required for *RTS1* activity, using 2D gel analysis of replication intermediates (Fig. 4*D*). Interestingly, the analysis of the Δ*pmt3* (SUMO) mutant strain detected a reduction in the *RTS1* pausing and termination similar to that observed in a Δ*rtf2* mutant strain. Furthermore, analysis of the Δ*rtf2* Δ*pmt3* double mutant established that the two mutations are nonadditive with regard to pausing and termination at the *RTS1* element. Interestingly, the Δ*pmt3* mutation does not produce the Δ*rtf2*-dependent increase in intensity of the descending Y-arc, suggesting that *S. pombe* does not require sumoylation for the establishment of slow-moving replication forks, but instead in the double mutant we observe that Δ*pmt3* partly suppresses the *rtf2*-dependent replication restart.

Discussion

In this study, we identify the Rtf2 factor, which mediates replication termination at the site-specific replication barrier *RTS1*, as the founding member of a family of proteins conserved from yeast to metazoan (Fig. 1). In an earlier study, we have shown that *rtf1*-null mutations lead to an abolishment of *RTS1* barrier activity; here we show that although the Δ*rtf2* mutation leads to a decrease of pause and termination signals, there is an increase in the signal from the large-Y intermediates formed when the replication forks have passed through the element (Fig. 2). We show that this increase in the intensity of large-Y intermediates is caused by replication restart involving the Srs2 helicase (Fig. 3). Here, the process of replication restart is directly observed at a replication barrier. However, we show that the repair polymerases Polη, Polκ, and Polζ are not involved in this replication restart; potentially, the restart could involve the replicative polymerases Polε and Polδ, but with altered processivity. Finally, we start to address the molecular mechanism by which Rtf2 acts; Rtf2 interacts with PCNA and, although a SUMO deletion mutation Δ*pmt3* causes a reduction in *RTS1* barrier activity, *rtf2* has no additive effects when combined with Δ*pmt3* in regard to pausing and termination activity at *RTS1* (Fig. 4), suggesting that they act together. In summary, our data suggest that Rtf2 acts downstream from Rtf1, converting a replication barrier into a replication termination site by stabilizing the stalled replication fork (Fig. 5).

Importantly, we are able to detect a strong nuclear signal of 13Myc and -GFP tagged Rtf2 using both direct detection and immunostaining (Fig. 4*A*). We also observe a slow growth and elongated-cell phenotype when the Δ*rtf2* mutation is combined with Δ*rqh1* and a slight sensitivity to metyl methane sulfonate (MMS) in the Δ*rtf2* mutant background (Figs. S5 and S6). Thus, although the molecular events that we describe here could be specific to *RTS1*, it is more likely that Rtf2 has a more general function during DNA replication. Potentially, this function could be either in preventing replication restart when converging replication forks terminate between firing origins, or in stabilizing replication forks that have collided with transcription forks. Finally, the fact that Rtf2 is part of a family of proteins phylogenetically conserved from yeast to metazoan also suggests a more general role for the defined Rtf2 activity.

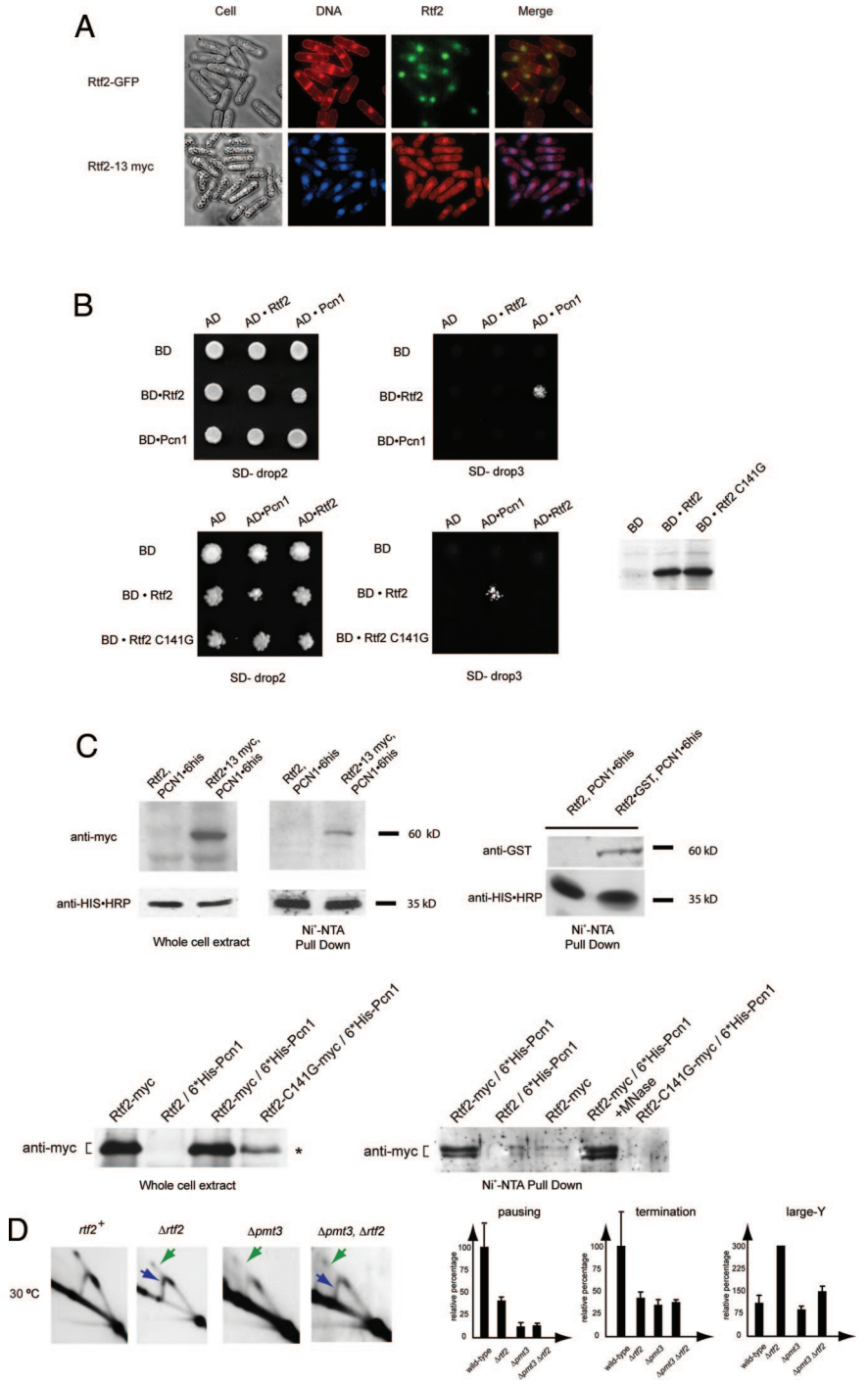

Fig. 4. Rtf2 in a nuclear PCNA-interacting protein. (*A*) The subcellular localization of Rtf2 was determined by direct fluorescence of live GFP-tagged Rtf2 cells (TISP86) and by immunostaining of glutaraldehyde-fixed 13Myc-tagged Rtf2 cells (TISP81). First column, DIC pictographs. Second column, Hoechst 33258 (live cells, *Upper*) and DAPI (fixed cells, *Lower*)-stained cells for detection of DNA. Third column, GFP fluorescence (*Upper*) and anti-Myc TRITC-conjugated anti-mouse IgG immunostained cells (*Lower*). Fourth column, overlay of DNA and Rtf2 signals. (*B*) A two-hybrid analysis uncovers a weak interaction between PCNA (*S. pombe* Pcn1) and Rtf2 that is abolished by the Rtf2-C141G amino acid substitution. (*Left*) the *S. cerevisiae* reporter strain (AH109) was transformed with the indicated pairs of Gal4 activation domain (AD) and Gal4 DNA-binding domain (BD) plasmids. Plasmids are listed above the panels. AD indicates that the plasmid only contains the Gal4 activation domain, whereas the AD·Rtf2 (pTAK22) and AD·Pcn1 (pTAK273) plasmids encode the activation domain fused to Rtf2 and PCNA, respectively. Plasmids are listed left of the panels; BD indicates that the plasmid only contains the Gal4 DNA-binding domain, whereas BD·Rtf2 (pTAK26) and BD·Pcn1 (pTAK276) plasmids encode the DNA-binding domain fused to Rtf2 and PCNA, respectively. Strains were grown on media (SD-drop2, −Leu, −Trp) selecting only for the plasmids and media (SD-drop3, −Leu, −Trp, −His) where cells only grow if an interaction between the plasmid-encoded fusion proteins is occurring. (*Right*) pBD·Rtf2 plasmid containing the Rtf2-C114G mutation (pTE202) is coexpressed with the AD·Rtf2 (pTAK22) and AD·Pcn1 (pTAK273) plasmids encoding the activation domain fused to Rtf2 and Pcn1, respectively. (*C*) PCNA pull-down experiments detect an interaction between PCNA and Rtf2. (*Upper*) A plasmid (pREP4X-MRG-*6xhis-pcn1*) containing His_6-tagged PCNA was transformed into Rtf2-13Myc (TISP81), Rtf2-GST (TISP38), or nontagged Rtf2 strains (JZ264). The strains were cultivated at 33 °C, and cell extracts were made, and pull-down experiments were performed by using a Ni^{2+}–NTA–resin. Tagged Rtf2 (60 kDa) was detected by Western blot analysis using anti-c-Myc monoclonal antibody or polyclonal anti-GST antibody. (*Left*) Analysis of both whole extracts and pull-down material. (*Right*) Displays experiments using only pull-down material. (*Lower Left*) Whole-cell extracts. (*Lower Right*) Ni^{2+}–NTA–agarose pull-down experiment. First and second lanes, positive and negative controls. Third lane, pull-down from a strain carrying a nontagged version of PCNA verifies that Rtf2 does not interact with Ni^{2+}–NTA–agarose. Fourth lane, MNase treatment does not affect the pull-down, thus the pull-down is not caused by DNA interactions. Fifth lane, the Rtf2-C141G RING-finger mutation abolishes the Pcn1 interaction. (*D*) (*Left*) Epistasis analysis of the Δ*pmt3* and Δ*rtf2* mutations. *RTS1* replication intermediates (pBZ142) in wild-type (JZ472), Δ*pmt3* (JN629), or Δ*rtf2* (SC10) single-mutant strains and the Δ*rtf2* Δ*pmt3* (TISP247) double-mutant strain were analyzed by 2D gel. (*Right*) Graphs display the intensity of the observed pause, termination, and large-Y signals relative to those of the wild-type signals. The experiment was done at 30 °C because the Δ*pmt3* causes a slight temperature sensitivity.

Materials and Methods

Strain and Plasmid Construction. Strains used are listed in Table S1. Standard methods were used for strain construction (25). GFP-, GST-, or 13Myc-tagged Rtf2 strains were constructed as described in ref. 26. For each of the tagged alleles, it was verified by using the genetic assay described in Fig. 1*A* that Rtf2 activity was not affected. Rtf2 cDNA was amplified by using a one-step RT-PCR kit (Qiagen) and cloned into the pCRII vector (Invitrogen).

Quantification of Sporulation. Unless stated otherwise, colonies were grown on sporulation (PMA^+) medium at 30 °C for 3 days. For each strain, the percentage of sporulation for three independent colonies was quantified as described in ref. 27.

Determination of the Subcellular Localization of Rtf2. Strains carrying either 13Myc- (TISP81) or GFP-tagged Rtf2 (TISP86) were grown in YEA medium at 25 °C. Hoechst 33258 (1 μg/mL; Sigma) was used for chromosomal DNA staining. Indirect immunofluorescence microscopy imaging was performed as described in ref. 28. Chromosomal DNA in fixed cells was stained by DAPI [4′,6-diamino-2-phenylindole: 1× working stock; 1 μg/mL DAPI, 1 mg/mL *p*-phenylenediamine, which acts as antifade, 50% (vol/vol) glycerol].

Yeast Two-Hybrid Interaction Assay. The Gal4-based Matchmaker Two-Hybrid System 3 (BD Clontech) assay was performed according to the manufacturer's instructions. *pcn1* cDNA and *rtf2* cDNA fragments were cloned into the pGADT7 vector tagging the Gal4 activation domain (plasmids pTAK273 and pTAK22,

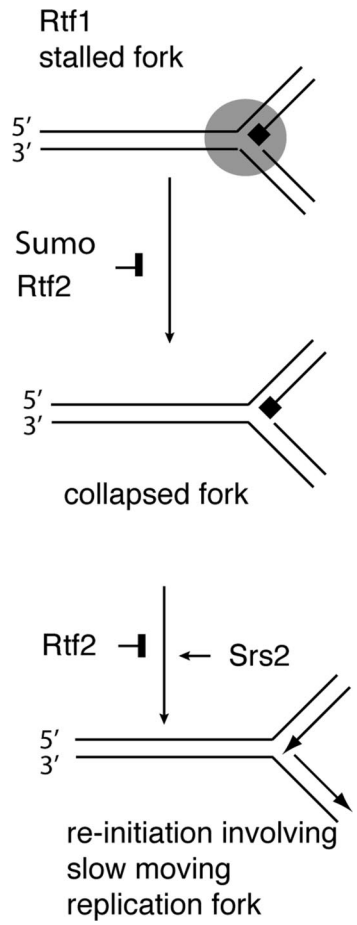

Fig. 5. Model of Rtf2 role in site-specific replication termination. Replication forks are stalled by Rtf1 at *RTS1* and are stabilized in a SUMO- and Rtf2-dependent manner. In the absence of Rtf2 the stalled replication fork collapses, and Srs2 act to reinitiate replication involving slow-moving forks.

respectively) and into pGBKT7 tagging the Gal4 DNA-binding domain (pTAK276 and pTAK26, respectively). The fusion proteins were subsequently coexpressed in pairs in *S. cerevisiae* strain AH109. Drop assays were performed by using SD-drop2 (−Leu and −Trp), SD-drop3 (−Leu, −Trp, and −His) plates. Plates were incubated for 4 days at 30 °C and subsequently photographed.

2D Gel Analysis of Replication Intermediates. Strains were transformed with a plasmid pBZ142 or pSC11 encoding *RTS1* or *RTS1* region B only, respectively. Cultures of the obtained strains were grown by using leucine dropout medium (25). DNA from logarithmically growing cultures was purified, and replication intermediates were isolated and digested with restriction enzymes SacI and PstI, and subsequently analyzed on 2D gels as described elsewhere (13, 29). A ^{32}P-labeled probe specific to the 0.8-kb *RTS1* element was used for the Southern analysis.

Pcn1 Pull-Down Assay. *S. pombe* strains TISP38 and TISP81 harboring pREP4 or pREP4XH6-PCN1 (30) were grown in uracil dropout medium. One liter of exponentially growing cells (OD_{600} = 0.8) was harvested and resuspended in lysis buffer [50 mM Tris·HCl (pH 8.0), 120 mM NaCl, 0.5% Nonidet P-40, protease inhibitor mixture (Roche), 50 mM NaF, 0.1 mM $Na3VO_4$, 10 mM β-glycophosphate, 0.05% sodium deoxycholate, 10% (vol/vol) glycerol]. Cells were broken by vortexing with 400- to 600-μm glass beads (Sigma). Whole-cell extracts were obtained by centrifuging at 15,000 × *g* for 30 min. Supernatants were incubated with Ni^{2+}–nitrilotriacetic acid (NTA) resin beads (Qiagen) overnight. The beads were washed 3 times with buffer A [50 mM Tris·HCl (pH 8.0), 150 mM NaCl, 0.5% Nonidet P-40, 0.05% sodium deoxycholate, 10% glycerol, and 20 mM imidazol]. Bound proteins were eluted from the Ni^{2+}-resin by using buffer B (as buffer A but excluding the 500 mM imidazol). The eluted proteins were separated on a 12% SDS/polyacrylamide gel and analyzed by Western blot analysis using either anti-GST antibody (1:5,000; Cancer Research), anti-c-Myc antibody (1:5,000, Invitrogen; and 4A6, 1:2,500, Upstate), anti-His_6 antibody (1:1,000; Invitrogen), or anti-PCNA antibody (PC10, 1:1,000; Santa Cruz) as primary antibodies. Subsequently, incubation with secondary horseradish peroxidase-conjugated anti-mouse or anti-rabbit IgG antibodies (1:5,000; Amersham) and the Super Signal peroxidase solution (Pierce) were used for detection.

ACKNOWLEDGMENTS. We thank Dr. Katsunori Tanaka (University of Shimane), Dr. Fekret Osman (University of Oxford), and Dr. Stuart MacNeill (University of St. Andrews) for kindly providing strains and plasmids for this study. We also thank our colleagues at the Marie Curie Research Institute for helpful suggestions and interactions. This work was supported by the Marie Curie Cancer Care (J.Z.D.) and the Association of International Cancer Research (J.Z.D.).

1. Lopes M, et al. (2001) The DNA replication checkpoint response stabilizes stalled replication forks. *Nature* 412:557–561.
2. Tercero JA, Diffley JF (2001) Regulation of DNA replication fork progression through damaged DNA by the Mec1/Rad53 checkpoint. *Nature* 412:553–557.
3. Sogo JM, Lopes M, Foiani M (2002) Fork reversal and ssDNA accumulation at stalled replication forks owing to checkpoint defects. *Science* 297:599–602.
4. Paques F, Haber JE (1999) Multiple pathways of recombination induced by double-strand breaks in *Saccharomyces cerevisiae*. *Microbiol Mol Biol Rev* 63:349–404.
5. Doe CL, Dixon J, Osman F, Whitby MC (2000) Partial suppression of the fission yeast rqh1(−) phenotype by expression of a bacterial Holliday junction resolvase. *EMBO J* 19:2751–2762.
6. Kai M, Wang TS (2003) Checkpoint responses to replication stalling: Inducing tolerance and preventing mutagenesis. *Mutat Res* 532:59–73.
7. Prakash S, Johnson RE, Prakash L (2005) Eukaryotic translesion synthesis DNA polymerases: Specificity of structure and function. *Annu Rev Biochem* 74:317–353.
8. Heller RC, Marians KJ (2006) Replisome assembly and the direct restart of stalled replication forks. *Nat Rev Mol Cell Biol* 7:932–943.
9. Doe CL, Whitby MC (2004) The involvement of Srs2 in post-replication repair and homologous recombination in fission yeast. *Nucleic Acids Res* 32:1480–1491.
10. Eydmann T, et al. (2008) Molecular mechanism of Rtf1-mediated eukaryotic site-specific replication termination. *Genetics* 180:27–39.
11. Dalgaard JZ, Klar AJ (2001) A DNA replication-arrest site RTS1 regulates imprinting by determining the direction of replication at mat1 in *S. pombe*. *Genes Dev* 15:2060–2068.
12. Dalgaard JZ, Klar AJ (2000) *swi1* and *swi3* perform imprinting, pausing, and termination of DNA replication in *S pombe*. *Cell* 102:745–751.
13. Codlin S, Dalgaard JZ (2003) Complex mechanism of site-specific DNA replication termination in fission yeast. *EMBO J* 22:3431–3440.
14. Dalgaard JZ, Klar AJ (1999) Orientation of DNA replication establishes mating-type switching pattern in *S pombe*. *Nature* 400:181–184.
15. Marchler-Bauer A, et al. (2007) CDD: A conserved domain database for interactive domain family analysis. *Nucleic Acids Res* 35:D237–D240.
16. Wang SW, Goodwin A, Hickson ID, Norbury CJ (2001) Involvement of *Schizosaccharomyces pombe* Srs2 in cellular responses to DNA damage. *Nucleic Acids Res* 29:2963–2972.
17. Krejci L, et al. (2003) DNA helicase Srs2 disrupts the Rad51 presynaptic filament. *Nature* 423:305–309.
18. Veaute X, et al. (2003) The Srs2 helicase prevents recombination by disrupting Rad51 nucleoprotein filaments. *Nature* 423:309–312.
19. Pfander B, Moldovan GL, Sacher M, Hoege C, Jentsch S (2005) SUMO-modified PCNA recruits Srs2 to prevent recombination during S phase. *Nature* 436:428–433.
20. Branzei D, et al. (2006) Ubc9- and mms21-mediated sumoylation counteracts recombinogenic events at damaged replication forks. *Cell* 127:509–522.
21. Borden KL (1998) RING fingers and B boxes: Zinc-binding protein–protein interaction domains. *Biochem Cell Biol* 76:351–358.
22. Stelter P, Ulrich HD (2003) Control of spontaneous and damage-induced mutagenesis by SUMO and ubiquitin conjugation. *Nature* 425:188–191.
23. Frampton J, et al. (2006) Postreplication repair and PCNA modification in *Schizosaccharomyces pombe*. *Mol Biol Cell* 17:2976–2985.
24. Hoege C, Pfander B, Moldovan GL, Pyrowolakis G, Jentsch S (2002) RAD6-dependent DNA repair is linked to modification of PCNA by ubiquitin and SUMO. *Nature* 419:135–141.
25. Moreno S, Klar A, Nurse P (1991) Molecular genetic analysis of fission yeast *Schizosaccharomyces pombe*. *Methods Enzymol* 194:795–823.
26. Bahler J, et al. (1998) Heterologous modules for efficient and versatile PCR-based gene targeting in *Schizosaccharomyces pombe*. *Yeast* 14:943–951.
27. Miyata M, Doi H, Miyata H, Johnson BF (1997) Sexual cofloculation by heterothallic cells of the fission yeast *Schizosaccharomyces pombe* modulated by medium constituents. *Antonie Van Leeuwenhoek* 71:207–215.
28. Hagan IM, Hyams JS (1988) The use of cell division cycle mutants to investigate the control of microtubule distribution in the fission yeast *Schizosaccharomyces pombe*. *J Cell Sci* 89:343–357.
29. Brewer BJ, Fangman WL (1987) The localization of replication origins on ARS plasmids in *S. cerevisiae*. *Cell* 51:463–471.
30. Reynolds N, Warbrick E, Fantes PA, MacNeill SA (2000) Essential interaction between the fission yeast DNA polymerase delta subunit Cdc27 and Pcn1 (PCNA) mediated through a C-terminal p21(Cip1)-like PCNA binding motif. *EMBO J* 19:1108–1118.
31. Brzovic PS, Rajagopal P, Hoyt DW, King MC, Klevit RE (2001) Structure of a BRCA1–BARD1 heterodimeric RING–RING complex. *Nat Struct Biol* 8:833–837.